agronomy

MDPI

Article

IIIVmrMLM Provides New Insights into the Genetic Basis of the Agronomic Trait Variation in Chickpea

Maria Duk [1,2], Alexander Kanapin [1], Ekaterina Orlova [1] and Maria Samsonova [1,*]

[1] Institute for Physics and Mechanics, Peter the Great St. Petersburg Polytechnic University, 29, Polytekhnicheskaya Str., 195251 St. Petersburg, Russia; duk@mail.ioffe.ru (M.D.); a.kanapin@gmail.com (A.K.); osyaginae@mail.ru (E.O.)
[2] Sector for Theory of Solids, Ioffe Institute, 26, Polytekhnicheskaya Str., 194021 St. Petersburg, Russia
* Correspondence: m.g.samsonova@gmail.com; Tel.: +7-812-290-9645

Abstract: Chickpea is a staple crop for many nations worldwide. Modeling genotype-by-environment interactions and assessing the genotype's ability to contribute adaptive alleles are crucial for chickpea breeding. In this study, we evaluated 12 agronomically important traits of 159 accessions from the N.I. Vavilov All Russian Institute for Plant Genetic Resources collection. These included 145 landraces and 13 cultivars grown in different climatic conditions in Kuban (45°18′ N and 40°52′ E) in both 2016 and 2022, as well as in Astrakhan (46°06′ N and 48°04′ E) in 2022. Using the IIIVmrMLM model in multi-environmental mode, we identified 161 quantitative trait nucleotides (QTNs) with stable genetic effects across different environments. Furthermore, we have observed 254 QTN-by-environment interactions with distinct environment-specific effects. Notably, five of these interactions manifested large effects, with R^2 values exceeding 10%, while the highest R^2 value for stable QTNs was 4.7%. Within the protein-coding genes and their 1 Kb flanking regions, we have discerned 22 QTNs and 45 QTN-by-environment interactions, most likely tagging the candidate causal genes. The landraces obtained from the N.I Vavilov All Russian Institute for Plant Genetic Resources collection exhibit numerous favorable alleles at quantitative trait nucleotide loci, showing stable effects in the Kuban and Astrakhan regions. Additionally, they possessed a significantly higher number of Kuban-specific favorable alleles of the QTN-by-environment interaction loci compared to the Astrakhan-specific ones. The environment-specific alleles found at the QTN-by-environment interaction loci have the potential to enhance chickpea adaptation to specific climatic conditions.

Keywords: IIIVmrMLM; agronomic traits; chickpea; GWAS; gene-by-environment interaction; multi-locus models

Citation: Duk, M.; Kanapin, A.; Orlova, E.; Samsonova, M. IIIVmrMLM Provides New Insights into the Genetic Basis of the Agronomic Trait Variation in Chickpea. *Agronomy* **2024**, *14*, 1762. https://doi.org/10.3390/agronomy14081762

Academic Editors: Fernando Martinez-Moreno, Magdalena Ruiz, María B. Picó and María-José Díez

Received: 25 June 2024
Revised: 3 August 2024
Accepted: 5 August 2024
Published: 12 August 2024

1. Introduction

At present, GWAS (Genome-Wide Association Study) is considered the gold standard for detecting associations between genomic variants and traits [1]. A classical implementation of a single-trait GWAS tests each marker at a time for association with a phenotype [2]. The widespread usage of MLM (mixed linear) models improved the prediction of true associations by removing confounding effects introduced by population structure and accession relatedness [3,4]. The application of these models is hindered by the Bonferroni correction used to correct for multiple testing, proving overly restrictive in identifying certain associations with complex traits in crops [5]. Bonferroni correction leads to a strong overestimation of the type I error, thereby missing true effects, i.e., decreasing the power of the experiment as the number of hypotheses grows [6].

In addressing this issue, the multi-locus MLM models have been developed to test all markers within the frame of one linear model while simultaneously estimating all marker effects [7–9]. An important advantage of such models over single-locus GWAS is their ability to detect quantitative trait nucleotides (QTNs) with marginal effects, where the significance threshold set by the Bonferroni correction is too stringent.

Most GWAS models only consider additive marker effects. However, dominance, gene-by-gene, and gene-by-environment interactions also play a crucial role in shaping the genetic architecture of complex traits in plants. Current methods for detecting these interactions are computationally complex and only estimate the effects of allele substitution and allele interaction, considering the specific control of the polygenic background [10,11]. This leads to the inadequate control of the polygenic background and confounding in the estimation of the marker effect.

The IIIVmrMLM model [12,13] has been developed to address methodological challenges in detecting various interactions between alleles, genes, and environments, while also providing an unbiased estimation of their genetic effects. This multi-locus MLM model simultaneously estimates the effects of all genes and interactions, using a computationally less complex approach that involves calculating only three compressed estimates instead of a large number of variance components. Additionally, the IIIVmrMLM model uses the expectation maximization empirical Bayes algorithm to estimate all effects within one multi-locus model, and significant QTNs are further evaluated via likelihood ratio tests. This methodology theoretically ensures the accurate detection of loci and an unbiased estimation of their effects, making IIIVmrMLM a suitable choice for detecting associations between genes, traits, and environments.

As sessile organisms, plants demonstrate remarkable phenotypic plasticity [14]. Both genotype and environment contribute to the phenotypic variation in a trait, and these factors interact at times in complex and non-additive ways [15]. The combination of genes and the environment plays a crucial role in shaping the plant's response to changes in the environment, particularly in terms of important agricultural traits. Identifying these interactions can help in developing plant varieties that are better equipped to withstand climate changes [16].

Chickpea, the second most extensively cultivated food legume, supplies important nutritional nitrogen and high-caliber protein for roughly 15% of the global population [17,18]. In West Asia and the Indian subcontinent, chickpea stands out as the most widely consumed legume. Its cultivation spans across 50 nations globally, as it has increasingly become a fundamental component of the Mediterranean diet. Currently, the proportion of grain legume crops, such as chickpeas, in EU agricultural regions is minimal, while chickpea production in Russia is on the rise [19,20]. Russia plays a significant role as a major global supplier of chickpeas, accounting for approximately 25% of the global chickpea trade prior to 2022. Furthermore, there has been a notable increase in crop breeding efforts, with six out of the 14 registered varieties in Russia being developed within the past five years.

The application of omics technologies in breeding has proven effective on several crops. However, progress in chickpea genomics has been relatively slow compared to other crop species such as cereals. A shift has occurred in the last decade through the large-scale characterization of germplasm and the construction of a pan-genome [21–23]. A combined analysis of the available phenotypic and genotypic data identified candidate markers for many agronomic important traits, including tolerance to abiotic and biotic stresses [21–31]. Breeding strategies based on genomic prediction to enhance crop productivity have been proposed [22,32,33].

Chickpea was often relegated to marginal lands where various abiotic stresses such as water deficits, extreme temperatures, short growing seasons, and poor soils contribute to limited yield potential [34]. For instance, drought decreases chickpea yield in the world by 50%, and losses caused by extreme temperature account for up to 20% [35]. In view of this, the cultivation of highly productive and climate change-resilient chickpea genotypes is essential given the evolving consumer demands, agricultural practices, and the need to adapt to a broader climatic range. The current elite high-yielding chickpea cultivars lack genetic and adaptive variation, highlighting the necessity to broaden the genetic base for continuous variety development. This entails exploring primitive landraces collected prior to the Green Revolution and the application of modern breeding methods to tap into the aforementioned significant additional source of genetic variation.

In the early 20th century, Nikolay Vavilov meticulously gathered chickpea land-races, which are currently preserved at the N.I. Vavilov All-Russian Institute of Plant Genetic Resources (VIR) in St. Petersburg, Russia. Previously, we interrogated these data to reveal marker–trait association using single-trait GWAS [31]. To gain a better understanding of the genetic factors behind variations in agronomic traits in chickpeas, we conducted GWAS using the IIIVmrMLM program. This program enables the detection of both quantitative trait nucleotides (QTNs) and quantitative environment interactions (QTN-by-environment interactions, QEIs).

2. Materials and Methods

2.1. Plant Growing and Phenotyping

A total of 159 chickpea genotypes were specifically chosen from the collection at the N.I. Vavilov All-Russian Institute of Plant Genetic Resources (VIR) in St. Petersburg, Russia (see Table S23). Within this dataset, 145 landraces and 13 elite cultivars were carefully included. These landraces, which were gathered by N.I. Vavilov during his expeditions in the 1920s–1930s, represent a valuable historical and genetic resource. To categorize the samples, six geographic regions were identified based on their geographical proximity: Mediterranean (MED), Lebanon (LEB), South of Russia (RUSS), Turkey (TUR), Uzbekistan (UZB), and India (IND).

Phenotyping of the chickpea accessions was conducted at two OSs of the VIR, the Kuban OS in 2016 and 2022 and the Astrakhan OS in 2022. The Kuban OS is located in the steppe zone of the Kuban–Priazovskaya lowlands, approximately 80 km from the Caucasus foothills. The soil at this location is predominantly black-rich, with a fertile layer depth of 140–150 cm and a slightly alkaline pH. The humus horizon is 130–170 cm thick, with humus content ranging from 3.6% to 4.6%. The climate is characterized as temperate continental, with hot summers, sub-optimal rainfall, and high fluctuation in climatic parameters. The sum of active temperatures above 10 °C ranges from 3200 to 3400 °C, and the average annual precipitation is 565 mm.

The Astrakhan OS is situated in the Caspian lowlands in the southern part of Astrakhan Oblast. The region experiences a continental climate, which is the driest in the European territory of the Russian Federation. It has substantial thermal resources, with a sum of active temperatures above 10 °C ranging from 3000 to 3500 °C. Annual precipitation varies from 180 to 200 mm, with the majority (70–75%) occurring in the warm season. The combination of low precipitation and high temperatures contributes to the dryness of both the air and soil. The predominant soils in the area are brown semi-desert soils with a humus content of 1.1%, light particle size distribution, low soil absorption capacity, and a neutral pH.

The duration of daylight likely had minimal impact on the plant development in the Kuban and Astrakhan regions, as both locations are situated at approximately the same latitude.

Both sites followed similar agronomic practices, with the exception that crops at the Astrakhan OS were irrigated seven times a day. A drip irrigation system was used at the recommended rate for irrigating vegetable crops, with an irrigation norm of 50.4 m^3 per season, or 400 m^3 per hectare. Sowing took place in late April 2022, with harvesting occurring in late July to early August. At both locations, the accessions were planted in a randomized complete block design with one replicate. Crop maintenance involved manual weeding (four times), mechanized row spacing treatment (two times), and the application of the pesticide "Stomp" (three times at a concentration of 4.5 L/ha). Urea (45% N) was used as fertilizer at a concentration of 800 g/L.

Throughout the vegetative period, we conducted measurements on 12 phenological and morphological traits (Table S1), including plant height (PH), the height of the first pod attachment (HFP), the number of primary branches (NPB), the number of secondary branches (NSB), plant dry weight with pods (PWwP), pod weight per plant (PoW), pod number per plant (PoNP), 100 seed weight (100SW), leaf size (LS), days from emergence to

flowering start (DFst), flowering duration (DF), and days from emergence to full maturation (Dmat). Our analysis encompassed six plants for each accession.

2.2. DNA Sequencing and Variant Calling

The DNeasy Plant Mini Kit (Qiagen, Germantown, MD, USA) was used to extract DNA from collected leaves. DNA was sequenced at the BGI (Shenzhen, China) using the Illumina technology, generating paired-end reads of 150 bp. A total of 7700 Gbp of raw data comprising about 26 billon reads with an average of 25× coverage or about 37 Gbp per sample were generated. Reads were processed and aligned to the chickpea reference genome assembly ASM33114v1 with bwa-mem using default parameters [36]. NGSEP [37] version 4.0. was used to call variants. A total of 96,354,236 biallelic SNPs were further filtered with VCF tools [38] to retain SNPs with minor allele frequency (MAF) > 5% and genotype call-rate > 85%. A total of 171,038 SNPs passed all filters and remained for further analysis.

2.3. Genetic Data Analyses

The genetic structure in the dataset was evaluated using the ADMIXTURE software v.1.3.0 [39]. The analyses were performed for K values ranging from 2 to 7. The linkage disequilibrium (LD) decay was estimated using squared Pearson's correlation coefficient (r2). The PopLDdecay [40] version 3.4.1 was run to calculate r^2 in a 500 kb window. The LD decay was calculated based on R^2 and the distance for each pair of SNPs using an R script in accordance with Hill–Weir approximation [41]. We applied the Mann–Whitney–Wilcoxon test [42] to make group comparisons. Two-way analysis of variance was carried out using the R function aov() from library stats.

2.4. GWAS

The genome-wide association analysis was performed using IIIVmrMLM program [13] run in Multi_env mode with parameters svpal = 0.01 and SearchRadius = 20. Suggested QTNs (SUG) were QTNs with LOD $\geq$ 3.0, significant QTNs (SIG) are QTNs with the Bonferroni corrected *p*-values calculated from LOD score using $\chi 2$ distribution. Candidate genes containing either QTNs or QEIs in gene bodies or within 1 kb flanking regions were annotated using The Pulse Crop Database https://www.pulsedb.org/Analysis/1869759 (accessed on 15 April 2024).

3. Results

3.1. Evaluation of Phenotypes

In 2022, 159 chickpea accessions were grown at two VIR (N.I. Vavilov All-Russian Institute for Plant Genetic Resources) outstations (OSs): the Astrakhan OS (46°06′ N, 48°04′ E, altitude 24 m) and the Kuban OS (45°18′ N, 40°52′ E, altitude 138.9 m). Additionally, the same chickpea accessions were also grown at the Kuban OS in 2016.

The hottest agricultural year across environments was at the Astrakhan OS in 2022 (Table S2). The sum of active temperatures above 10 °C was 3419. This exceeds the values at the Kuban OS in 2016 and 2022 by 346 °C and 525 °C, correspondingly (Tables S3 and S4). The wettest agricultural year across environments was at the Kuban OS in 2022, with annual precipitation equal to 744 mm, which exceeds the values at the same station in 2016 by 128 mm and at the Astrakhan OS by 547 mm.

In every year and at each location, all accessions were evaluated for 12 traits related to yield, vegetative growth and flowering time (Table S1, Figure 1a). In both regions, yield-related traits, i.e., plant dry weight with pods (PWwP), the weight of pods per plant (PoW), the number of pods per plant (PoNP), and a 100 seed weight (100SW) have the largest coefficient of variation (see Table S5). The variability of most other traits in the dataset is also large, ranging from 20 to 30%. The values for traits related to yield and vegetative growth, except for the height of the first pod attachment (HFP) and 100SW, are significantly different between environments (p value < 0.05). Specifically, a similar number

of days was required for plants to start flowering in 2022, but not in 2016 (see Table S5). However, at the Astrakhan OS, the flowering phenophase lasted longer than at the Kuban OS. The period from emergence to full maturation was also much longer at the Kuban OS than at the Astrakhan OS (refer to Figure 1a).

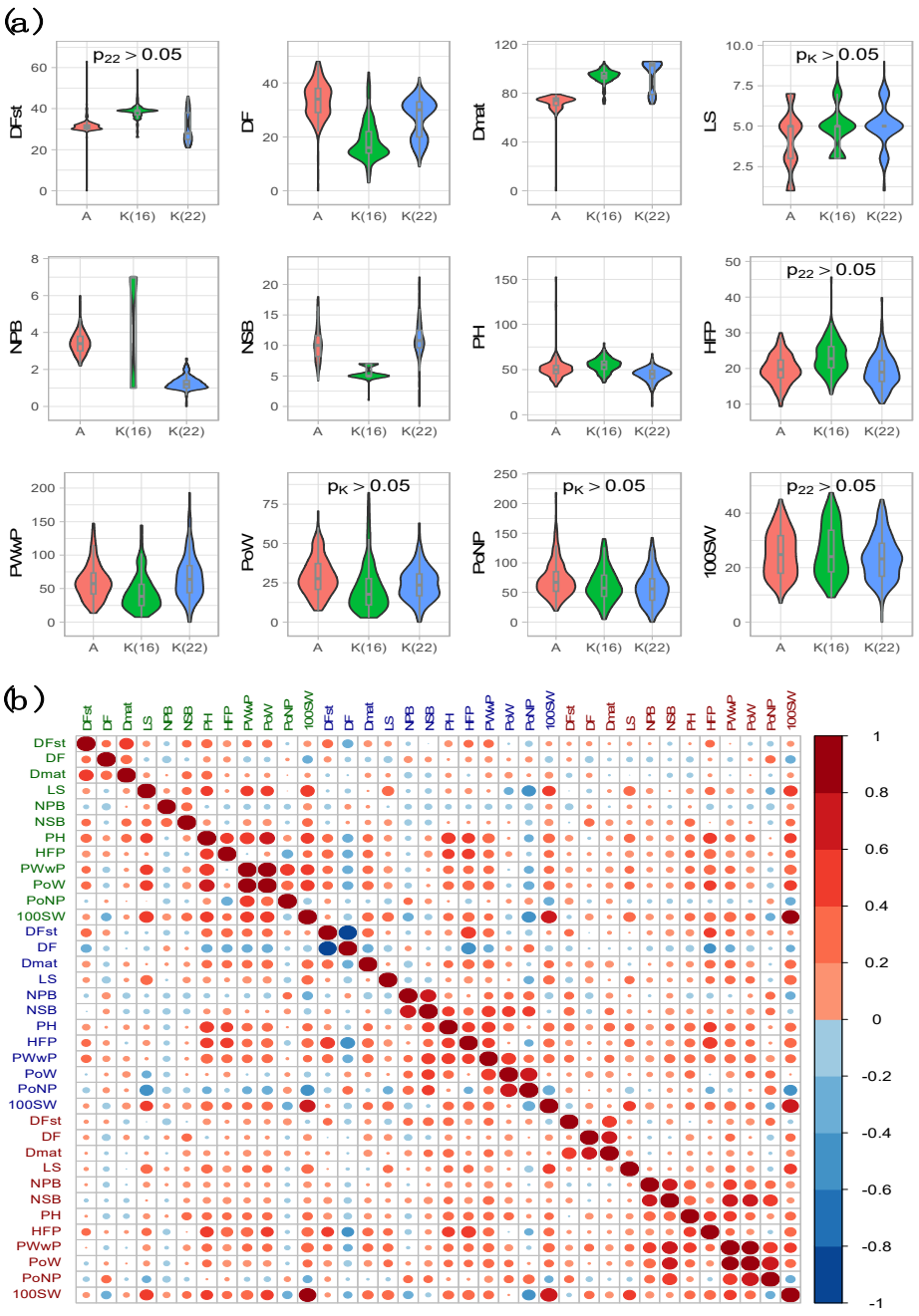

Figure 1. Evaluation of the phenotypes. (**a**) Violin plots showing trait data collected at the Kuban and the Astrakhan outstations. *p*-values > 5% (Mann–Whitney test) define statistically insignificant differences between trait values. p22, as shown at the top, stands for *p*-values obtained when comparing traits from Kuban and Astrakhan regions in 2022, while pK stands for *p*-values in the 2016 and 2022 trait comparisons in the Kuban region. The labels are: A for the Astrakhan OS, K(16)—the Kuban OS in 2016, K(22)—the Kuban OS data in 2022. The abbreviations for the trait names are listed in Table S1 and Table A1. (**b**) Pearson correlation coefficient for traits (Table S6); green labels are for Kuban in 2016, blue labels are for Kuban in 2022, and red labels are for Astrakhan.

In both Astrakhan and Kuban regions, the traits PoNP, PoW, and PWwP are correlated, as shown in Figure 1b and Table S6. However, these traits are not correlated across different environments, indicating a significant influence of the growing conditions on the phenotype. On the other hand, 100SW and HFP show correlation across different environments, suggesting that the growing conditions have minimal impact on these traits. In each environment, PoNP, PoW, and PWwP demonstrate a correlation with NSB, which is a major contributor to plant yield. Notably, in the data collected from Astrakhan and Kuban in 2016, both the time from emergence to flowering (DFst) and the flowering phase (DF) are significantly correlated with the time from germination to full maturity (Dmat). However, this correlation is not observed in accessions grown in Kuban in 2022, indicating a strong environmental effect on these traits (Table S6).

The effects of genotype, environment and genotype-by-environment interaction were statistically significant for traits related to yield and vegetative growth (Table S7). The estimates for gene-by-environment interaction were highly significant, suggesting that genotype performance should be assessed in each specific environment. In the case of flowering traits and LS, all plants belonging to the same accession exhibit the same trait value precluding the estimation of the genotype-by-environment interaction effects. However, the effects of genotype and environment are statistically significant for all these traits (Table S7).

3.2. Population Analysis

The genetic makeup of the dataset was determined using a group of 171,038 SNPs. In tune with previous findings, the principal component analysis did not show any distinct separation among the samples based on their geographical origin [31,43]. The lowest cross-validation error in the ADMIXTURE analysis occurred when the number of populations was set to three (K = 3). However, the errors at K = 4 and K = 5 were only slightly larger, suggesting that these three population splits are the most preferable (see Figure 2a,c,d). The ADMIXTURE analysis shows that accessions can be divided into six almost geographically isolated groups: Indian (IND), Turkish (TUR), Mediterranean (MED), Lebanese (LEB), Uzbek (UZB), and South Russian (RUS). Further examination reveals that the ADMIXTURE patterns of geographically adjacent populations (Indian and Uzbek, as well as Turkish and Mediterranean) are more similar than the patterns of populations located farther away. This likely reflects the history of chickpea migration after domestication [36].

LD decays fast in the dataset, reaching half of a maximum r^2 value at a distance of 50 kb (Figure 2b). Of note, the LD decay observed in this study was much faster than those detected for Desi and Kabuli chickpea cultivars in other datasets (340 kb and 330 kb correspondingly), as well as for the cultivated soybean (150 kb) [22,44].

3.3. Identification of QTNs and QEIs Associated with Phenotypic Traits

The IIIVmrMLM method allows us to calculate the QTNs and QEIs separately, thus dividing markers into groups, namely (a) markers with stable effects across different environments, and (b) markers associated with phenotypic effects in selected environments only.

We have identified 161 QTNs and 254 QEIs as the significant markers for 12 different phenotypic traits (refer to Tables S8 and S9). On average, QTNs accounted for approximately 19.6% of the variation across the different traits, while QEIs explained an average of 48.6% of the variation, ranging from 27.6% to 63% for different traits (see Table 1). This indicates that the independent quantitative effects of markers were generally lower than the effects of their interaction with the environment.

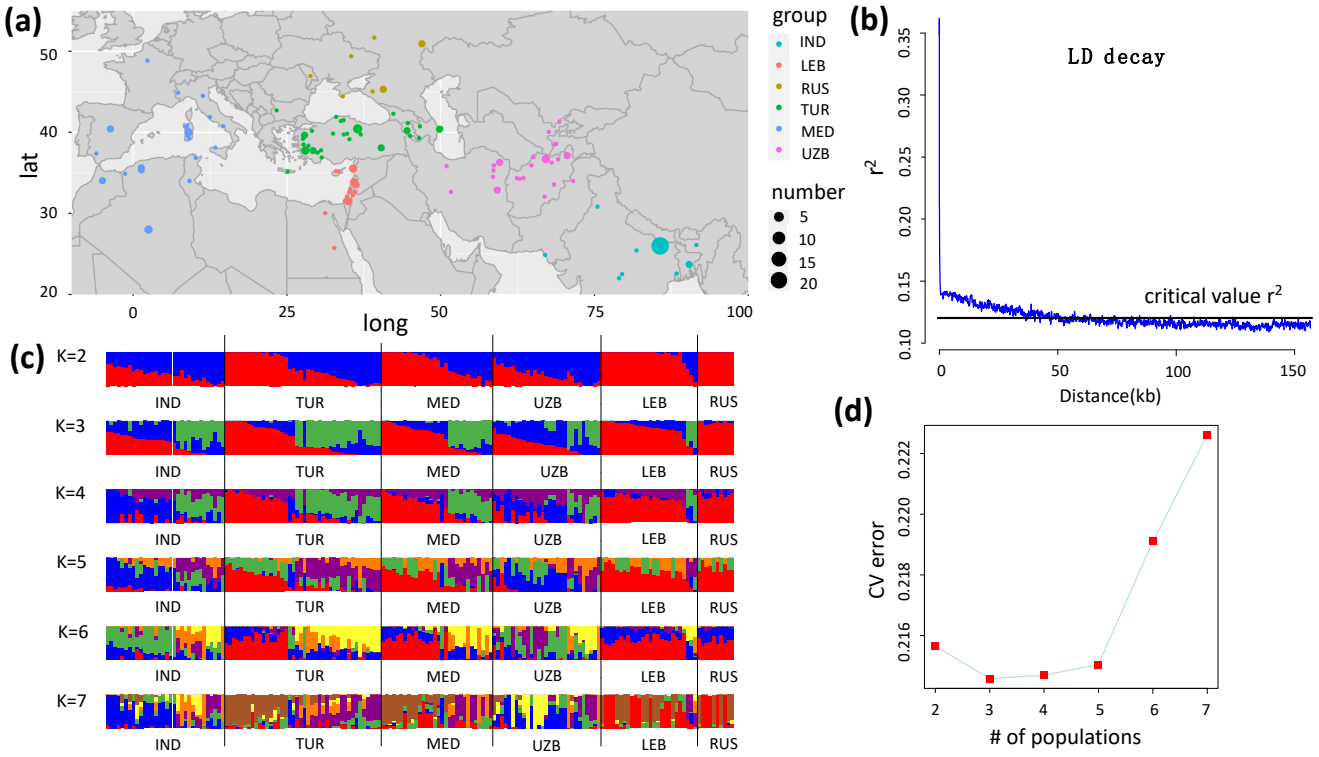

Figure 2. Sample origins and population analysis. (**a**) Sample collection sites. (**b**) LD decay in the dataset. (**c**,**d**) Population structure inferred with ADMIXTURE. ADMIXTURE results generated with different numbers of populations (K = 2–7). Each sample is represented by a vertical stacked bar; colors correspond to different ancestral populations.

Table 1. Percentage of trait variation explained by QTNs and QEIs. * Abbreviations of trait names are as shown in Tables S1 and A1.

Trait Name *	Type	Total Variation Explained (%)	Marker Explaining the Largest Variation in a Trait	R^2 (%)
DF	QTN	15.9	Ca5_21845257	1.9
	QEI	43.5	Ca2_495917	2.2
DFst	QTN	26.4	Ca7_22036380	4.2
	QEI	38.1	Ca7_18941640	6.0
Dmat	QTN	13.6	Ca3_17850594	2.5
	QEI	50.8	Ca4_22649405	5.0
LS	QTN	25.7	Ca8_12966424	3.3
	QEI	40.3	Ca2_27433383	17.2
NPB	QTN	19.0	Ca6_47226273	2.8
	QEI	48.8	Ca7_20175638	2.8
NSB	QTN	14.3	Ca6_31708450	1.5
	QEI	63.0	Ca4_29141628	14.8
PH	QTN	26.7	Ca4_22648344	4.6
	QEI	27.6	Ca4_6063638	8.0
HFP	QTN	24.4	Ca4_27164303	3.8
	QEI	48.3	Ca7_14064521	27.3
PWwP	QTN	15.2	Ca5_44207860	2.1
	QEI	55.2	Ca3_19996983	21.6

Table 1. *Cont.*

Trait Name *	Type	Total Variation Explained (%)	Marker Explaining the Largest Variation in a Trait	R^2 (%)
PoW	QTN	19.0	Ca4_25847872	3.1
	QEI	61.0	Ca5_21206336	11.4
PoNP	QTN	16.3	Ca4_43416762	2.2
	QEI	52.7	Ca3_27518251	5.4
100SW	QTN	18.2	Ca7_32823511	2.3
	QEI	54.2	Ca4_33626689	4.6

The QTN Ca4_22648344 linked to plant height explained 4.6% of the variation, while Ca7_14064521 associated with the HFP trait explained the largest percentage of variation at 27.3%. Likewise, four other QEIs, namely Ca2_27433383, Ca4_29141628, Ca5_21206336 and Ca3_19996983 associated with leaf size (LS), number of secondary branches (NSB), pod weight per plant (PoW) and plant weight with pods (PWwP), respectively, also explained more than 10% of the trait variation (Table 1).

Quantitative trait loci are primarily located on chromosomes 1, 4, 5, and 6 (Figure 3a). QTNs associated with traits PoW, NPB, DF, and Dmat, which showed the most variation between environments, were identified on chromosomes 4, 5, and 6 (Figure 3b,c). Additionally, QTNs linked to these traits were also found on chromosomes 1, 2, and 7. The most QEIs are found on chromosomes 1, 4, and 7. QEIs for DF and Dmat traits are mainly located on chromosomes 1 and 4, also on chromosome 7. Few QTNs for the Dmat trait are on chromosome 6 compared to other traits. QEIs for PoW are on all chromosomes except 8.

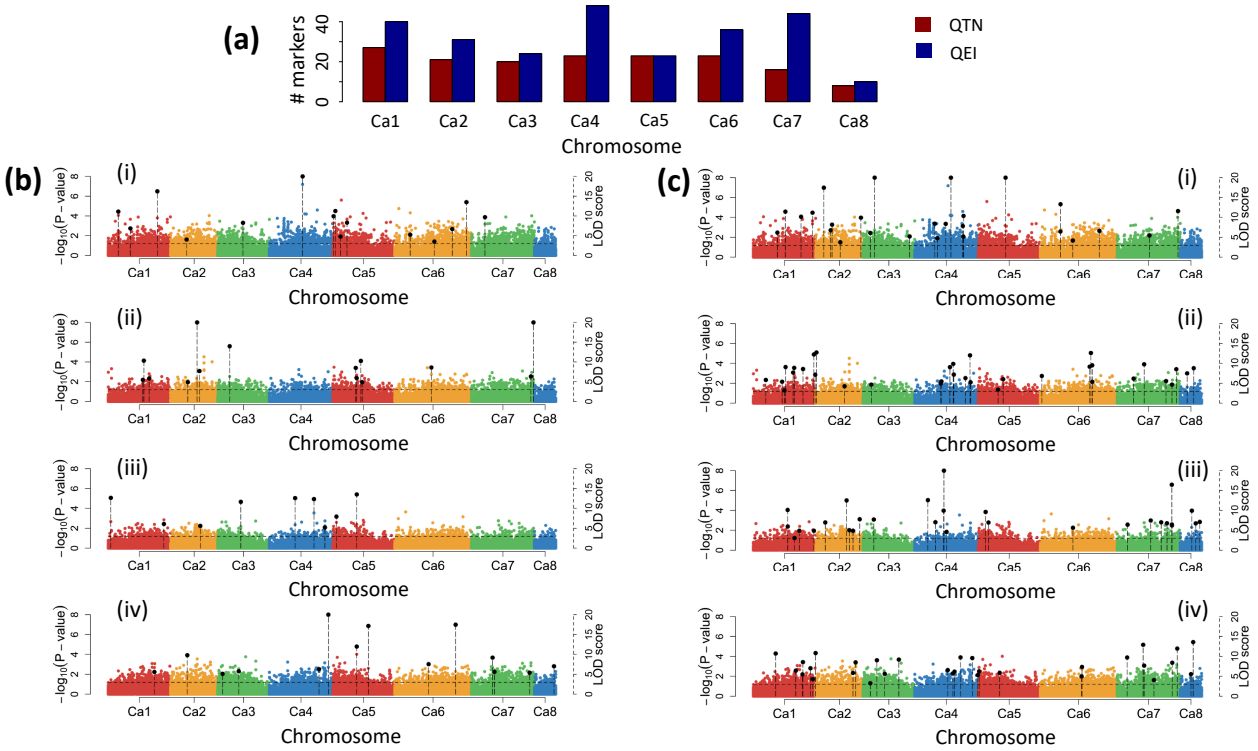

Figure 3. QTNs and QEIs associated with traits. (**a**) Number of markers found on each chromosome. (**b**) Manhattan plot displaying QTNs for PoW (**i**), DF (**ii**), Dmat (**iii**) and NPB (**iv**) across chromosomes. (**c**) Manhattan plot displaying QEIs for the aforementioned traits. The abbreviations of trait names are as shown in Table S1 and Table A1.

3.4. Known Genes around Predicted QTNs and QEIs

Within the protein-coding genes and their 1 Kb flanking regions, we found 22 QTNs and 45 QEIs, most likely tagging the candidate causal genes. Functional annotation was available for 13 QTN-harboring genes and 28 QEI-harboring genes (see Tables 2 and 3).

Table 2. QTNs located within protein-coding genes and their 1 Kb flanking regions. * Abbreviations of trait names are in Tables S1 and A1; ** gene body, *** 5′—upstream, **** 3′—downstream.

Trait Name *	QTN	Effect (Add)	R^2	Gene	QTN Position (bp)	Annotation	Function
100SW	Ca4_47959199	−0.1758	0.89	*Ca_10794*	GB **	BAG family molecular chaperone regulator 1	Chaperon
100SW	Ca5_8331723	−0.19	1.34	*Ca_18706*	GB	E3 ubiquitin-protein ligase MBR2	Flowering control, promotes degradation of the *FT* regulator [45]
DF	Ca1_27596774	−0.132	1.73	*Ca_25069*	864 bp, 5′ ***	carbon catabolite repressor protein 4 homolog 4-like	Regulator of circadian rhythms [46]
DF	Ca3_9196031	0.154	0.59	*Ca_20953*	824 bp, 3′ ****	probable xyloglucan glycosyltransferase 5	xyloglucan modification
DFst	Ca1_8374473	0.166	1.29	*Ca_08073*	303 bp, 3′ ****	ethylene-responsive transcription factor 1-like	Response to pathogens and salinity in plant [47]
DFst	Ca2_15613312	0.135	1.94	*Ca_18543*	440 bp, 3′	pentatricopeptide repeat-containing protein At2g33760	
HFP	Ca4_8807893	0.055	2.19	*Ca_08378*	GB	transcription factor bHLH106	Salt and low temperature response [48]
HFP	Ca6_53308665	0.141	1.73	*Ca_22925*	790 bp, 3′	UDP-glycosyltransferase 89B2	Transfer of a sugar onto a lipophilic acceptor [49]
HFP	Ca7_14294458	−0.133	1.18	*Ca_23043*	GB	peptidyl-prolyl cis-trans isomerase CYP37, chloroplastic	Regulation of the electron transport chain [50]
LS	Ca5_7212528	0.177	2.59	*Ca_21567*	GB	AP-5 complex subunit mu	Vesicle transport regulator [51]
NPB	Ca5_27676347	0.172	2.02	*Ca_08885*	92 bp, 3′	iron-sulfur assembly protein IscA-like 1, mitochondrial	Assembly of mitochondrial iron-sulfur proteins [52]
NSB	Ca1_22298342	0.13	0.93	*Ca_20631*	GB	40S ribosomal protein S28-1-like	
PoNP	Ca1_26015468	−0.121	1.42	*Ca_18590*	445 bp, 3′	triose phosphate/phosphate translocator, chloroplastic	Phosphate transport, light response [53]
PoW	Ca5_665190	0.144	1.05	*Ca_23223*	763 bp, 5′	ninja-family protein AFP2	Regulator of AREB/ABF transcription factors [54]

Table 3. QEIs located within protein-coding genes and their 1 Kb flanking regions. * Abbreviations of trait names are in Tables S1 and A1; ** K16—Kuban in 2016, K22—Kuban in 2022, A—Astrakhan, *** GB—gene body, 3′—downstream, 5′—upstream.

Trait Name *	QEI	Add env1 (K16) **	Add env2 (K22)	ADD env3 (A)	R^2	Gene	QTN Position	Annotation	Function
100SW	Ca2_15153528	0.096	−0.144	0.048	1.07	*Ca_18572*	28 bp, 3′	dof zinc finger protein DOF1.4-like	Abiotic stress tolerance [55]
100SW	Ca4_12413458	0.056	−0.1268	0.071	0.81	*Ca_04464*	GB ***	cyclic dof factor 1-like	Regulates a photoperiodic flowering response [56]
DF	Ca4_27283954	0.166	−0.048	−0.118	1.5	*Ca_20463*	695 bp, 3′	putative Ulp1 protease family catalytic domain-containing protein	SUMO protease [57]

Table 3. *Cont.*

Trait Name *	QEI	Add env1 (K16) **	Add env2 (K22)	ADD env3 (A)	R^2	Gene	QTN Position	Annotation	Function
DF	Ca7_37894908	0.06	−0.133	0.074	0.92	*Ca_16382*	GB	ubiquitin carboxyl-terminal hydrolase 2	Involved in the direct or indirect regulation of AUX/IAA proteins stability [58]
DFst	Ca3_22914338	−0.06	0.175	−0.113	1.76	*Ca_06215*	GB	pentatricopeptide repeat-containing protein At2g44880-like, partial	ABA hypersensitivity at germination, RNA editing [59]
DFst	Ca5_11805008	0.112	0.003	−0.115	0.95	*Ca_17114*	GB	cucumisin-like	Serine protease [60]
DFst	Ca7_25029782	0.113	0.035	−0.148	1.34	*Ca_23595*	GB	probable polygalacturonase	Polygalacturonases involved in cell separation in the final stages of pod shatter and in anther dehiscence [61]
Dmat	Ca1_26611572	0.147	−0.009	−0.138	1.43	*Ca_18616*	194 bp, 5′	WUSCHEL-related homeobox 9-like	Homeodomain transcription factor required for meristem growth and early development [62]
Dmat	Ca1_31837660	−0.098	0.009	0.089	0.62	*Ca_26401*	GB	cytokinin dehydrogenase 6-like	Catalyzes the oxidation of cytokinins [63]
Dmat	Ca3_8285781	−0.025	−0.137	0.162	1.62	*Ca_24378*	GB	homeobox-leucine zipper protein PROTODERMAL FACTOR 2-like	Regulator of shoot epidermal cell differentiation [64]
LS	Ca1_42237742	0.262	0.013	−0.275	6.31	*Ca_22678*	395 bp, 5′	transcription factor bHLH49-like	Involved in cell elongation regulation [65]
NPB	Ca4_25599443	0.117	0.011	−0.128	1.29	*Ca_16586*	GB	endochitinase A-like	Antifungal protection in crops [66]
NPB	Ca7_28494061	−0.091	−0.016	0.106	0.85	*Ca_18936*	183 bp, 3′	leucine-rich repeat extensin-like protein 4	Represent a link between the cell wall and plasma membrane [67]
NPB	Ca8_8247161	−0.017	0.123	−0.106	1.15	*Ca_11459*	GB	aspartic proteinase-like protein 2	Pathogen stress response [68]
PoNP	Ca1_3619635	−0.00	0.189	−0.189	2.34	*Ca_00444*	GB	protein MALE DISCOVERER 2-like	Involved in recognition female gametes after pollination [69]
PoNP	Ca3_1396781	−0.047	0.258	−0.212	3.75	*Ca_19418*	GB	protein DEHYDRATION-INDUCED 19 homolog 5-like	Involved in dehydration and salinity stress signaling pathways [70]
PoNP	Ca4_22873605	−0.131	−0.06	0.191	1.89	*Ca_14464*	518, bp 5′	putative disease resistance protein At3g14460	
PoNP	Ca5_17861341	−0.028	−0.143	0.17	1.65	*Ca_22848*	GB	aspartyl protease family protein At5g10770-like	aspartyl protease
PoNP	Ca6_47911283	−0.151	0.056	0.095	1.15	*Ca_23445*	GB	alanine aminotransferase 2-like	alanine aminotransferase
PoNP	Ca7_20945484	−0.035	0.175	−0.139	1.68	*Ca_14487*	863 bp, 3′	Retrovirus-related Pol polyprotein from transposon TNT 1-94	
PoW	Ca2_6214519	−0.249	0.024	0.225	3.56	*Ca_20925*	775 bp, 3′	fructose-bisphosphate aldolase 1, chloroplastic	Involved in photosynthesis [71]
PoW	Ca2_12581771	0.003	0.16	−0.163	1.64	*Ca_18081*	GB	ATP synthase subunit delta′, mitochondrial	[72]
PoW	Ca2_18976694	0.12	−0.014	−0.105	0.8	*Ca_15955*	GB	B3 domain-containing protein At5g42700-like	AP2/B3-like transcriptional factor [73]
PoW	Ca2_34943639	−0.067	0.2	−0.139	2.07	*Ca_16876*	GB	tRNA (guanine(26)-N(2))-dimethyltransferase	Posttranscriptional modification of tRNA [74]
PoW	Ca3_8932912	−0.351	0.047	0.304	6.83	*Ca_25280*	GB	alcohol dehydrogenase-like 6	alcohol dehydrogenase

Table 3. *Cont.*

Trait Name *	QEI	Add env1 (K16) **	Add env2 (K22)	ADD env3 (A)	R^2	Gene	QTN Position	Annotation	Function
PoW	Ca6_15593063	0.038	−0.222	0.184	2.66	*Ca_05341*	GB	protein EMBRYO DEFECTIVE 514	[75]
PWwP	Ca3_19996983	0.103	0.589	−0.692	21.59	*Ca_09401*	GB	proteasome subunit beta type-4-like	
PWwP	Ca4_24437355	−0.218	−0.019	0.2367	2.69	*Ca_20867*	194 bp, 3′	cyclase-associated protein 1	Increases the rate of nucleotide exchange on actin [76]

3.5. Superior Genotypes for Key Traits

The development of high-yielding and early-maturing chickpea varieties is limited by a significant reduction in genetic and adaptive variation. Chickpea landraces provide a wide range of genetic variations that have not been thoroughly explored and utilized systematically by breeders [77,78].

To identify genotypes with high yield and early maturation among the VIR landraces we calculated two statistics, namely (1) the number of favorable alleles of the QTN and QEI loci controlling Dmat and yield-related traits (PoW, PoNP, PWwP and 100SW), and (2) the "trait improvement" (TI) score as the difference between the number of favorable alleles and the alleles negatively affecting the trait for each accession. Since QEI loci are environment-specific, the repertoire of the QEI alleles in samples was assessed for each environment separately.

The number of favorable alleles for the QTNs associated with the Dmat trait does not exceed four in the samples (Table S10). The highest TI score of 4 or 5 is calculated for 14 samples. The number of favorable alleles for the QTN loci associated with yield-related traits ranges from 17 to 26 (Table S11). Twenty two samples had a TI score higher than 10, and two of them have the highest TI score of 13.

In the Kuban region, there are more favorable alleles of the QEI loci for the Dmat trait and fewer alleles with negative effects compared to the Astrakhan OS (Tables S12–S14). The highest TI score for landraces grown in the Kuban region in 2016 and 2022 ranges from 4 to 9, with 26 accessions scoring in this interval at each of the outstations (Tables S12 and S13). In the Astrakhan region, only four landraces have positive TI scores, with a value not exceeding 3 (Table S14).

A similar situation was observed for the QEI loci associated with yield-related traits: in the Kuban region, 21 accessions in 2016 and 11 in 2022 showed the highest value of TI score in the interval from 6 to 16, with the number of favorable alleles ranging from 29 to 40 (Tables S15 and S16). However, in Astrakhan, a large number of favorable alleles (from 25 to 32) is counterbalanced by an equally large number of alleles characterized by a negative effect. As a result, only five samples produced a positive TI score value (Table S17).

Landraces VIR1171, VIR0603, VIR0620, and VIR0668 grown at the Kuban OS in 2016 are characterized by high TI scores for both QTN and QEI loci associated with the Dmat trait. However, we found only two such landraces, namely, VIR0620 and VIR0799 cultivated at the Kuban OS in 2022 (Table S18). In addition, the VIR0230, VIR0244, VIR0030 and VIR0042 landraces at the Kuban OS in 2016, VIR0637 at the Kuban OS in 2022, as well as VIR0855 at the Astrakhan OS show high TI values for the QTNs and QEIs related to productivity.

High TI score values for QEI loci associated with the Dmat and yield-related traits are observed in two landraces, namely VIR0241 and VIR0918 at the Kuban OS in 2016 and 2022, respectively (Table S19).

4. Discussion

In recent years, mixed linear models have been extensively utilized to predict genomic regions linked to crucial traits in chickpeas [22,24,25,31,79]. However, the majority of these models [3,4,80] merely address the additive effects of markers and fail to estimate

dominance effects or gene-by-environment interactions. Importantly, the IIIVmrMLM model [12,13] utilized in this study enables the comprehensive evaluation of these effects.

Cultivars are evaluated based on their performance when grown in different environments [81,82]. Traits important for commercial agriculture, such as yield and maturity, often vary significantly between environments due to genotype-by-environment interactions. Therefore, it is essential to model these interactions and assess a genotype's ability to provide adaptive alleles for the successful breeding of resilient and sustainable crop varieties [77].

In this study, 159 accessions from the VIR collection, including 145 landraces and 13 cultivars, were planted in three different environments. The first two environments were the Kuban outstation in 2016 and 2022, and the third was the Astrakhan OS in 2022. In 2022 at the Kuban outstation, daily temperatures were lower compared to 2016, and precipitation levels were higher. The Astrakhan OS experienced the hottest and driest agricultural conditions across all environments (see Tables S2–S4 for details).

The evaluation of 12 important agronomic traits (Table S1) revealed significant variation within a single environment and across different environments (Table S5, Figure 1a). The most pronounced variation across environmental gradients was observed for productivity and phenological traits, suggesting a genotype-by-environment interaction. To comprehend the genetic factors responsible for trait variation across different environments, we utilized the IIIVmrMLM program in Multi_env (multi-environment) mode.

We have confidently identified a total of 161 QTNs with stable genetic effects across various environments and 256 QEIs with environment-specific effects (Tables S8 and S9). Collectively, both QTNs and QEIs account for a significant proportion of the variation across traits (Table 1).

Twenty two QTNs and 45 QEIs are linked to protein-coding genes, likely identifying potential causal genes (see Tables 2 and 3). The functions of many of these genes are known. For instance, Ca5_8331723, which is associated with 100SW, is located within the *Ca_18706* gene for E3 ubiquitin-protein ligase MBR2. This gene promotes the degradation of the Flowering Locus T regulator in *Arabidopsis* [45] (Table 2). The QTNs Ca1_27596774 and Ca1_8374473, which impact phenological traits, are found in the flanking regions of Ca_25069 and *Ca_08073* genes, respectively. These genes control circadian rhythm [46] as well as the response to pathogens and salinity [47]. The QTN Ca4_8807893, associated with the HFP trait, is located in the *Ca_08378* gene, which encodes the transcription factors involved in responding to unfavorable environmental conditions [48]. The QTNs Ca6_53308665 and Ca1_26015468, associated with HFP and PoNP, respectively, are downstream of the *Ca_22925* and *Ca_18590* genes, which control sugar [49] and phosphate transport [53]. QTN Ca5_665190, associated with PoW, is upstream of the *Ca_23223* gene implicated in hormone signaling [54].

Quantitative trait loci such as Ca7_37894908, Ca7_25029782 and Ca1_31837660 (see Table 3), associated with phenological traits, are located within genes that control AUX/IAA protein stability, cell separation during pod formation [58,61], and the oxidation of cytokinins [63], respectively. The QEIs Ca1_26611572 and Ca3_8285781, associated with the time from germination to full maturation (i.e., Dmat), map to the *Ca_18616* and *Ca_24378* genes. These genes encode a transcription factor participating in the regulation of meristem growth [62] and a homeobox-leucine zipper protein PROTODERMAL FACTOR 2-like (Table 3), respectively. Incidentally, PROTODERMAL FACTOR 2 regulates the differentiation of shoot epidermal cells in *Arabidopsis* [64].

The QEI Ca1_42237742, associated with leaf size, is upstream of the *Ca_22678* gene involved in the regulation of cell elongation [65]. The QEI Ca7_28494061, associated with NPB, is located 183 bp downstream of the *Ca_18936* gene, which encodes leucine-rich repeat extensin-like protein 4. This might coordinate processes in the cell wall, as leucine-rich extension receptors are known to do [67].

Ca1_3619635, which is located within the *Ca_00444* gene involved in gamete recognition, is associated with the number of pods. The recognition of female gametes after

pollination is crucial for successful seed formation [69]. Another QEI, Ca4_24437355, associated with the weight of plants with pods, is downstream of the *Ca_20867* gene involved in actin dynamics [76].

According to the recent findings [83], only 4 QTNs and 5 QEIs were found to overlap with the QTNs identified using Super, FarmCPU, and Blink models of the GAPIT package (Table S20). One of these QTNs, Ca3_8285781, which is associated with NSB, falls into the *Ca_24378* encoding PROTODERMAL FACTOR 2-like. The limited overlap between the results of these two analyses can be attributed to GAPIT identifying associated markers for each environment separately, while IIIVmrMLM in Multi_env mode predicts associations for the three environments simultaneously.

The comparison of GWAS hits with genomic regions from previous studies reveals that 48 QTNs and 88 QEIs intersect within the LD limits (50 kb) of QTNs identified in studies [21,22] (Tables S21 and S22). Although different studies assess slightly different traits, it is not surprising that many matched QTNs are associated with various traits. For instance, the study by Varshney et al. [21] measured days to 50% flowering instead of the Dmat, DF, and DFst traits from our study. Nevertheless, most of the associated traits, while different, measure the same characteristics of the plant, such as 100 seed weight, yield per plant, harvest index, and the number of primary and secondary branches characterizing productivity.

This study definitively established that VIR landraces possess multiple favorable alleles of the QTN loci with stable effects in varying climatic conditions of the Kuban and Astrakhan regions (Refer to Tables S10 and S11). Furthermore, a greater number of Kuban-specific favorable alleles of the QEI loci compared to the Astrakhan-specific ones (See Tables S12–S17) was observed. The impact of the favorable alleles of the QEI loci associated with the Dmat trait in the Astrakhan region is undeniably additive (see Figure 4), but it is adequately balanced by an equivalent or even larger number of negative alleles, as sown in Table S14. Despite these findings, it was irrefutable that the accessions in the Astrakhan OS matured at a faster rate than those in the Kuban region (Figure 1a and Table S5), suggesting that the explanation for this observation likely lies within the gene-by-gene interactions.

The analysis reveals negative correlations between maturation time (the Dmat trait) and several beneficial alleles for Astrakhan-specific QEI loci and loci specific for Kuban in 2016 (Figure 4). Conversely, a positive correlation is observed between productivity traits and the number of favorable alleles for most markers and traits, except for the PoW and 100SW traits measured at the Kuban OS in 2016. In these cases, the correlation was found to be statistically insignificant, with p-values equal to 0.66 and 0.41, respectively. The identified markers' additive effect on most traits suggests that accessions carrying more favorable alleles are conducive to breeding through the pyramiding of loci.

Large-effect quantitative trait loci (QEIs) such as Ca2_27433383, Ca4_29141628, Ca5_21206336, and Ca3_19996983 (see Table 1) can be incorporated into marker-assisted selection programs, while markers with minor effects are more likely to be utilized in genomic selection (GS) in combination with markers with large effects. Previously GS models have been employed for the prediction of yield traits in chickpea [32,33]. In this context, the environment-specific alleles of the QEI loci (Table S9) are particularly significant, as breeders can utilize them to develop varieties with improved adaptation to specific climatic conditions.

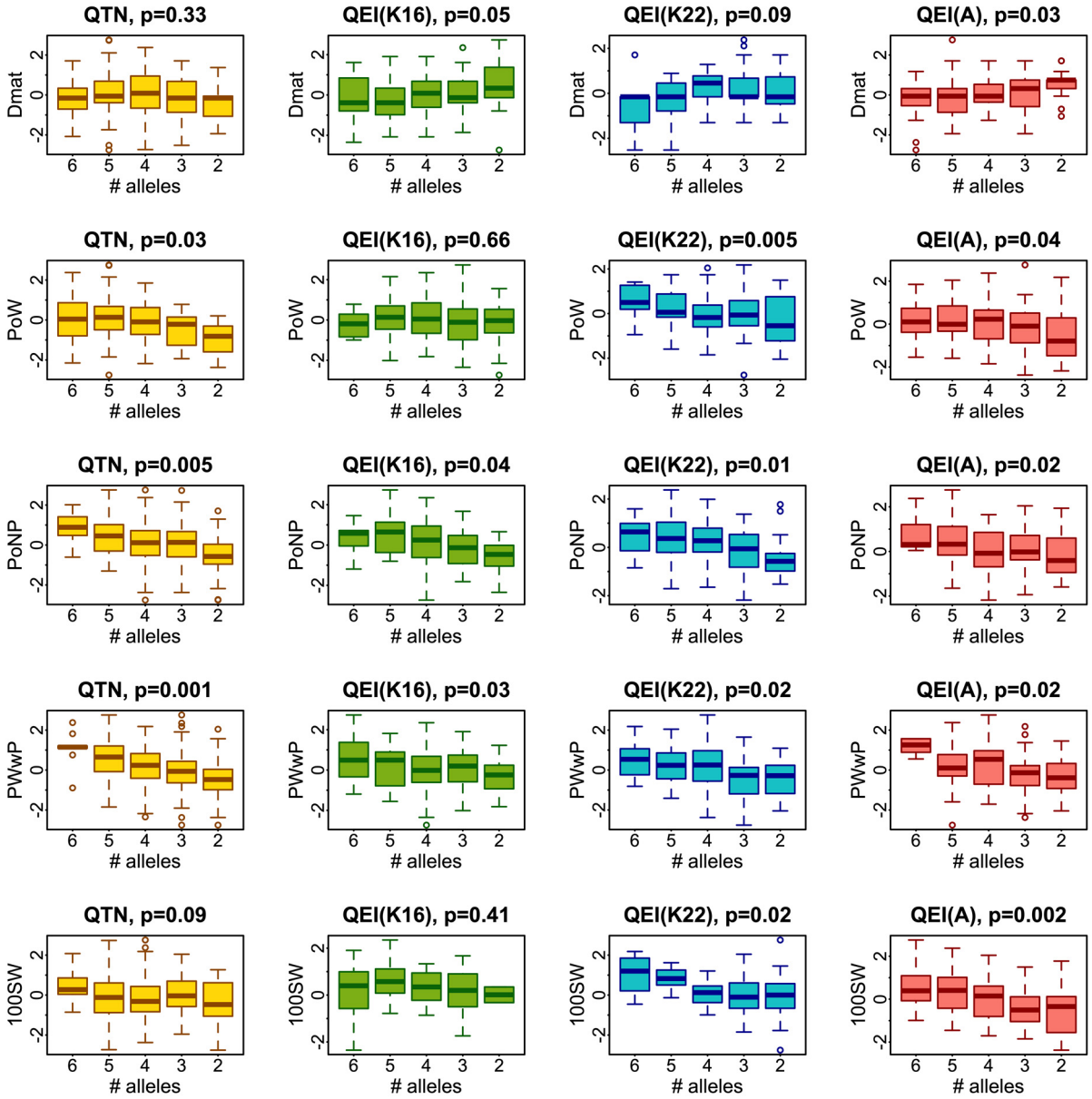

Figure 4. Box plots depict the relationship between the number of favorable alleles and the normalized trait phenotypes. Abbreviations for trait names are as listed in Table S1 and Table A1, with K16 representing Kuban 2016, K22 representing Kuban 2022, and A representing Astrakhan.

5. Conclusions

The genetic and phenotypic variation present in chickpea landraces has yet to be comprehensively explored. This study aims to expand the genetic diversity of chickpea by identifying landraces with adaptive and favorable alleles that control maturity and yield-related traits, with a specific focus on the VIR landraces. The assessment of traits in varying environments in the Kuban and Astrakhan regions revealed significant variation across environmental gradients, indicating genotype-by-environment interactions. To thoroughly examine stable and environment-specific effects, the IIIVmrMLM model was employed. The results showed that the VIR landraces possess numerous favorable alleles of the QTN loci, with stable effects in all tested environments. Importantly, they demonstrate a greater abundance of Kuban-specific alleles of the QEI loci compared to the Astrakhan-specific ones. The annotation of the genetic repertoire of favorable alleles in landraces is fundamental and imperative as the first step towards their integration into modern breeding programs.

Supplementary Materials: The following supporting information can be downloaded at: https://www.mdpi.com/article/10.3390/agronomy14081762/s1, Table S1: Abbreviations of trait names; Table S2: Agroclimatic data for Astrakhan in 2022; Table S3: Agroclimatic data for Kuban in 2016; Table S4: Agroclimatic data for Kuban in 2022; Table S5: Descriptive statistics for traits; Table S6: Trait correlations within and across environments; Table S7: Analysis of variance; Table S8: List of QTNs detected with IIIVmrMLM; Table S9: List of QEIs detected with IIIVmrMLM; Table S10: TI score and a number of favorable alleles for QTNs associated with the Dmat trait.; Table S11: TI score and a number of favorable alleles for QTNs associated with yield-related traits; Table S12: TI score and a number of favorable alleles for QEIs associated with Dmat traits in Kuban in 2016; Table S13: TI score and a number of favorable alleles for QEIs associated with Dmat traits in Kuban in 2022; Table S14: TI score and a number of favorable alleles for QEIs associated with Dmat traits in Astrakhan; Table S15: TI score and a number of favorable alleles for QEIs associated with yield-related traits in Kuban in 2016; Table S16: TI score and a number of favorable alleles for QEIs associated with yield-related traits in Kuban in 2022; Table S17: TI score and a number of favorable alleles for QEIs associated with yield-related traits in Astrakhan; Table S18: Samples with high TI values for QNT and QEI loci associated with traits; Table S19: Samples with high TI score values for both Dmat and yield-related traits; Table S20: QTNs and QEIs detected by IIIVmrMLM and GAPIT; Table S21: Comparison of QTN hits with genomic regions discovered in previous studies; Table S22: Comparison of QEI hits with genomic regions discovered in previous studies; Table S23: Dataset summary statistics.

Author Contributions: Conceptualization, M.S.; Methodology, A.K.; Software, M.D.; Validation, A.K.; Formal analysis, E.O.; Investigation, M.D.; Writing—original draft preparation, M.S.; Writing—review and editing, M.S.; Visualization, M.D.; Supervision, M.S.; Project administration, E.O.; Funding acquisition, M.S. All authors have read and agreed to the published version of the manuscript.

Funding: This research was funded by the Russian Science Foundation, grant number 22-46-02004 (the identification of QTNs and QEIs, as well as superior genotypes for key traits), as well as by the Ministry of Science and Higher Education of the Russian Federation as part of a World-class Research Center program: Advanced Digital Technologies (contract No. 075-15-2022-311, dated 20 April 2022) (population analysis and the annotation of casual genes).

Data Availability Statement: The data analyzed in the manuscript are available on public repository Zenodo https://zenodo.org/records/10895525 (accessed on 15 April 2024).

Acknowledgments: All the authors would like to thank the St. Petersburg State Polytechnic University Centre for Supercomputing (https://scc.spbstu.ru/) for providing excellent computational resources and support for this project.

Conflicts of Interest: The authors declare no conflicts of interest.

Appendix A

Table A1. Abbreviations of trait names.

Abbreviation	Trait
NPB	Number of primary branches
NSB	Number of secondary branches
PH	Plant height, sm
HFP	Height to the first pod
PWwP	Plant dry weight with pods, g
PoW	Pod weight per plant, g
PoNP	Pod number per plant
100SW	100 seed weight, g
LS	Leaf size

References

1. Hayes, B. Genome-Wide Association Studies and Genomic Prediction. *Methods Mol. Biol.* **2013**, *1019*, 149–169. [CrossRef] [PubMed]
2. Gupta, P.K.; Kulwal, P.L.; Jaiswal, V. Association Mapping in Plants in the Post-GWAS Genomics Era. *Adv. Genet.* **2019**, *104*, 75–154. [CrossRef] [PubMed]

3. Kang, H.M.; Sul, J.H.; Service, S.K.; Zaitlen, N.A.; Kong, S.; Freimer, N.B.; Sabatti, C.; Eskin, E. Variance Component Model to Account for Sample Structure in Genome-Wide Association Studies. *Nat. Genet.* **2010**, *42*, 348–354. [CrossRef] [PubMed]
4. Lippert, C.; Listgarten, J.; Liu, Y.; Kadie, C.M.; Davidson, R.I.; Heckerman, D. FaST Linear Mixed Models for Genome-Wide Association Studies. *Nat. Meth* **2011**, *8*, 833–835. [CrossRef] [PubMed]
5. Zhang, Y.-M.; Jia, Z.; Dunwell, J.M. Editorial: The Applications of New Multi-Locus GWAS Methodologies in the Genetic Dissection of Complex Traits. *Front. Plant Sci.* **2019**, *10*, 100. [CrossRef] [PubMed]
6. Segura, V.; Vilhjálmsson, B.; Platt, A.; Korte, A.; Seren, Ü.; Long, Q.; Nordborg, M. An efficient multi-locus mixed-model approach for genome-wide association studies in structured populations. *Nat. Genet.* **2012**, *44*, 825–830. [CrossRef] [PubMed]
7. Wang, S.-B.; Feng, J.-Y.; Ren, W.-L.; Huang, B.; Zhou, L.; Wen, Y.-J.; Zhang, J.; Dunwell, J.M.; Xu, S.; Zhang, Y.-M. Improving Power and Accuracy of Genome-Wide Association Studies via a Multi-Locus Mixed Linear Model Methodology. *Sci. Rep.* **2016**, *6*, 19444. [CrossRef] [PubMed]
8. Wen, Y.-J.; Zhang, H.; Ni, Y.-L.; Huang, B.; Zhang, J.; Feng, J.-Y.; Wang, S.-B.; Dunwell, J.M.; Zhang, Y.-M.; Wu, R. Methodological Implementation of Mixed Linear Models in Multi-Locus Genome-Wide Association Studies. *Brief. Bioinform.* **2017**, *19*, 700–712. [CrossRef] [PubMed]
9. Zhang, Y.-W.; Tamba, C.L.; Wen, Y.-J.; Li, P.; Ren, W.-L.; Ni, Y.-L.; Gao, J.; Zhang, Y.-M. MrMLM v4.0.2: An R Platform for Multi-Locus Genome-Wide Association Studies. *Genom. Proteom. Bioinform.* **2020**, *18*, 481–487. [CrossRef] [PubMed]
10. Moore, R.; Casale, F.P.; Bonder, M.J.; Horta, D.; Franke, L.; Barroso, I.; Stegle, O.; BIOS Consortium. A Linear Mixed-Model Approach to Study Multivariate Gene–Environment Interactions. *Nat. Genet.* **2019**, *51*, 180–186. [CrossRef] [PubMed]
11. Sul, J.H.; Bilow, M.; Yang, W.-Y.; Kostem, E.; Furlotte, N.; He, D.; Eskin, E. Accounting for Population Structure in Gene-by-Environment Interactions in Genome-Wide Association Studies Using Mixed Models. *PLoS Genet.* **2016**, *12*, e1005849. [CrossRef] [PubMed]
12. Li, M.; Zhang, Y.-W.; Zhang, Z.-C.; Xiang, Y.; Liu, M.-H.; Zhou, Y.-H.; Zuo, J.-F.; Zhang, H.-Q.; Chen, Y.; Zhang, Y.-M. A Compressed Variance Component Mixed Model for Detecting QTNs and QTN-by-Environment and QTN-by-QTN Interactions in Genome-Wide Association Studies. *Mol. Plant* **2022**, *15*, 630–650. [CrossRef] [PubMed]
13. Li, M.; Zhang, Y.-W.; Xiang, Y.; Liu, M.-H.; Zhang, Y.-M. IIIVmrMLM: The R and C++ Tools Associated with 3VmrMLM, a Comprehensive GWAS Method for Dissecting Quantitative Traits. *Mol. Plant* **2022**, *15*, 1251–1253. [CrossRef] [PubMed]
14. Napier, J.D.; Heckman, R.W.; Juenger, T.E. Gene-by-Environment Interactions in Plants: Molecular Mechanisms, Environmental Drivers, and Adaptive Plasticity. *Plant Cell* **2022**, *35*, 109–124. [CrossRef] [PubMed]
15. Saltz, J.B.; Bell, A.M.; Flint, J.; Gomulkiewicz, R.; Hughes, K.A.; Keagy, J. Why Does the Magnitude of Genotype-by-environment Interaction Vary? *Ecol. Evol.* **2018**, *8*, 6342–6353. [CrossRef] [PubMed]
16. Raza, A.; Razzaq, A.; Mehmood, S.S.; Zou, X.; Zhang, X.; Lv, Y.; Xu, J. Impact of Climate Change on Crops Adaptation and Strategies to Tackle Its Outcome: A Review. *Plants* **2019**, *8*, 34. [CrossRef] [PubMed]
17. Abbo, S.; Berger, J.; Turner, N.C. Viewpoint: Evolution of Cultivated Chickpea: Four Bottlenecks Limit Diversity and Constrain Adaptation. *Funct. Plant Biol.* **2003**, *30*, 1081–1087. [CrossRef] [PubMed]
18. Jain, M.; Misra, G.; Patel, R.K.; Priya, P.; Jhanwar, S.; Khan, A.W.; Shah, N.; Singh, V.K.; Garg, R.; Jeena, G.; et al. A Draft Genome Sequence of the Pulse Crop Chickpea (*Cicer arietinum* L.). *Plant J.* **2013**, *74*, 715–729. [CrossRef] [PubMed]
19. Zotikov, V.I.; Vilyunov, S.D. Present-day breeding of legumes and groat crops in Russia. *Vavilov J. Genet. Breed.* **2021**, *25*, 381–387. [CrossRef] [PubMed]
20. Mahmood, F.; Shahzad, T.; Hussain, S.; Shahid, M.; Azeem, M.; Wery, J. Grain Legumes for the Sustainability of European Farming Systems. In *Sustainable Agriculture Reviews*; Lichtfouse, E., Ed.; Springer: Cham, Switzerland, 2018; Volume 32. [CrossRef]
21. Varshney, R.K.; Thudi, M.; Roorkiwal, M.; He, W.; Upadhyaya, H.D.; Yang, W.; Bajaj, P.; Cubry, P.; Rathore, A.; Jian, J.; et al. Resequencing of 429 Chickpea Accessions from 45 Countries Provides Insights into Genome Diversity, Domestication and Agronomic Traits. *Nat. Genet.* **2019**, *51*, 857–864. [CrossRef] [PubMed]
22. Varshney, R.K.; Roorkiwal, M.; Sun, S.; Bajaj, P.; Chitikineni, A.; Thudi, M.; Singh, N.P.; Du, X.; Upadhyaya, H.D.; Khan, A.W.; et al. A Chickpea Genetic Variation Map Based on the Sequencing of 3,366 Genomes. *Nature* **2021**, *599*, 622–627. [CrossRef]
23. Upadhyaya, H.D.; Bajaj, D.; Srivastava, R.; Daware, A.; Basu, U.; Tripathi, S.; Bharadwaj, C.; Tyagi, A.K.; Parida, S.K. Genetic Dissection of Plant Growth Habit in Chickpea. *Funct. Integr. Genom.* **2017**, *17*, 711–723. [CrossRef] [PubMed]
24. Upadhyaya, H.D.; Bajaj, D.; Narnoliya, L.; Das, S.; Kumar, V.; Gowda, C.L.L.; Sharma, S.; Tyagi, A.K.; Parida, S.K. Genome-Wide Scans for Delineation of Candidate Genes Regulating Seed-Protein Content in Chickpea. *Front. Plant Sci.* **2016**, *7*, 302. [CrossRef] [PubMed]
25. Bajaj, D.; Upadhyaya, H.D.; Das, S.; Kumar, V.; Gowda, C.L.L.; Sharma, S.; Tyagi, A.K.; Parida, S.K. Identification of Candidate Genes for Dissecting Complex Branch Number Trait in Chickpea. *Plant Sci.* **2016**, *245*, 61–70. [CrossRef] [PubMed]
26. Kujur, A.; Bajaj, D.; Upadhyaya, H.D.; Das, S.; Ranjan, R.; Shree, T.; Saxena, M.S.; Badoni, S.; Kumar, V.; Tripathi, S.; et al. Employing Genome-Wide SNP Discovery and Genotyping Strategy to Extrapolate the Natural Allelic Diversity and Domestication Patterns in Chickpea. *Front. Plant Sci.* **2015**, *6*, 162. [CrossRef] [PubMed]
27. Das, S.; Singh, M.; Srivastava, R.; Bajaj, D.; Saxena, M.S.; Rana, J.C.; Bansal, K.C.; Tyagi, A.K.; Parida, S.K. MQTL-Seq Delineates Functionally Relevant Candidate Gene Harbouring a Major QTL Regulating Pod Number in Chickpea. *DNA Res.* **2016**, *23*, 53–65. [CrossRef] [PubMed]

28. Ortega, R.; Hecht, V.F.G.; Freeman, J.S.; Rubio, J.; Carrasquilla-Garcia, N.; Mir, R.R.; Penmetsa, R.V.; Cook, D.R.; Millan, T.; Weller, J.L. Altered Expression of an FT Cluster Underlies a Major Locus Controlling Domestication-Related Changes to Chickpea Phenology and Growth Habit. *Front. Plant Sci.* **2019**, *10*, 824. [CrossRef] [PubMed]
29. Thudi, M.; Khan, A.W.; Kumar, V.; Gaur, P.M.; Katta, K.; Garg, V.; Roorkiwal, M.; Samineni, S.; Varshney, R.K. Whole Genome Re-Sequencing Reveals Genome-Wide Variations among Parental Lines of 16 Mapping Populations in Chickpea (*Cicer arietinum* L.). *BMC Plant Biol.* **2016**, *16*, 1–12. [CrossRef] [PubMed]
30. van-Oss, R.P.; Gopher, A.; Kerem, Z.; Peleg, Z.; Lev-Yadun, S.; Sherman, A.; Zhang, H.; Vandemark, G.; Coyne, C.J.; Reany, O.; et al. Independent Selection for Seed Free Tryptophan Content and Vernalization Response in Chickpea Domestication. *Plant Breed.* **2018**, *137*, 290–300. [CrossRef]
31. Sokolkova, A.; Bulyntsev, S.V.; Chang, P.L.; Carrasquilla-Garcia, N.; Igolkina, A.A.; Noujdina, N.V.; von Wettberg, E.; Vishnyakova, M.A.; Cook, D.R.; Nuzhdin, S.V.; et al. Genomic Analysis of Vavilov's Historic Chickpea Landraces Reveals Footprints of Environmental and Human Selection. *Int. J. Mol. Sci.* **2020**, *21*, 3952. [CrossRef] [PubMed]
32. Roorkiwal, M.; Rathore, A.; Das, R.R.; Singh, M.K.; Jain, A.; Srinivasan, S.; Gaur, P.M.; Chellapilla, B.; Tripathi, S.; Li, Y.; et al. Genome-Enabled Prediction Models for Yield Related Traits in Chickpea. *Front. Plant Sci.* **2016**, *7*, 1666. [CrossRef] [PubMed]
33. Li, Y.; Ruperao, P.; Batley, J.; Edwards, D.; Martin, W.; Hobson, K.; Sutton, T. Genomic Prediction of Preliminary Yield Trials in Chickpea: Effect of Functional Annotation of SNPs and Environment. *Plant Genome* **2022**, *15*, e20166. [CrossRef] [PubMed]
34. de la Peña, T.C.; Pueyo, J.J. Legumes in the Reclamation of Marginal Soils, from Cultivar and Inoculant Selection to Transgenic Approaches. *Agron. Sustain. Dev.* **2012**, *32*, 65–91. [CrossRef]
35. Kaloki, P.; Devasirvatham, V.; Tan, D.K.Y. *Chickpea Abiotic Ssresses: Combating Drought, Heat and Cold*; IntechOpen: London, UK, 2019. [CrossRef]
36. Li, H.; Durbin, R. Fast and Accurate Short Read Alignment with Burrows–Wheeler Transform. *Bioinformatics* **2009**, *25*, 1754–1760. [CrossRef] [PubMed]
37. Tello, D.; Gonzalez-Garcia, L.N.; Gomez, J.; Zuluaga-Monares, J.C.; Garcia, R.; Angel, R.; Mahecha, D.; Duarte, E.; Leon, M.d.R.; Reyes, F.; et al. NGSEP 4: Efficient and Accurate Identification of Orthogroups and Whole-Genome Alignment. *Mol. Ecol. Resour.* **2022**, *23*, 712–724. [CrossRef] [PubMed]
38. Danecek, P.; Auton, A.; Abecasis, G.; Albers, C.A.; Banks, E.; DePristo, M.A.; Handsaker, R.E.; Lunter, G.; Marth, G.T.; Sherry, S.T.; et al. The Variant Call Format and VCFtools. *Bioinformatics* **2011**, *27*, 2156–2158. [CrossRef] [PubMed]
39. Alexander, D.H.; Novembre, J.; Lange, K. Fast Model-Based Estimation of Ancestry in Unrelated Individuals. *Genome Res.* **2009**, *19*, 1655–1664. [CrossRef] [PubMed]
40. Zhang, C.; Dong, S.-S.; Xu, J.-Y.; He, W.-M.; Yang, T.-L. PopLDdecay: A Fast and Effective Tool for Linkage Disequilibrium Decay Analysis Based on Variant Call Format Files. *Bioinformatics* **2018**, *35*, 1786–1788. [CrossRef] [PubMed]
41. Hill, W.G.; Weir, B.S. Variances and Covariances of Squared Linkage Disequilibria in Finite Populations. *Theor. Popul.Biol* **1988**, *33*, 54–78. [CrossRef] [PubMed]
42. Mann, H.B.; Whitney, D.R. On a Test of Whether One of Two Random Variables Is Stochastically Larger than the Other. *Ann. Math Stat.* **1947**, *18*, 50–60. [CrossRef]
43. Igolkina, A.A.; Noujdina, N.V.; Vishnyakova, M.; Longcore, T.; von Wettberg, E.; Nuzhdin, S.V.; Samsonova, M.G. Historical Routes for Diversification of Domesticated Chickpea Inferred from Landrace Genomics. *Mol. Biol. Evol.* **2023**, *40*, msad110. [CrossRef] [PubMed]
44. Zhou, Z.; Jiang, Y.; Wang, Z.; Gou, Z.; Lyu, J.; Li, W.; Yu, Y.; Shu, L.; Zhao, Y.; Ma, Y.; et al. Resequencing 302 Wild and Cultivated Accessions Identifies Genes Related to Domestication and Improvement in Soybean. *Nat. Biotechnol.* **2015**, *33*, 408–414. [CrossRef] [PubMed]
45. Iñigo, S.; Giraldez, A.N.; Chory, J.; Cerdán, P.D. Proteasome-Mediated Turnover of Arabidopsis MED25 Is Coupled to the Activation of *FLOWERING LOCUS T* Transcription. *Plant Physiol.* **2012**, *160*, 1662–1673. [CrossRef] [PubMed]
46. Delis, C.; Krokida, A.; Tomatsidou, A.; Tsikou, D.; Beta, R.A.; Tsioumpekou, M.; Moustaka, J.; Stravodimos, G.; Leonidas, D.D.; Balatsos, N.A.; et al. AtHESPERIN: A novel regulator of circadian rhythms with poly(A)-degrading activity in plants. *RNA Biol.* **2016**, *13*, 68–82. [CrossRef] [PubMed] [PubMed Central]
47. Lee, J.H.; Hong, J.P.; Oh, S.K.; Lee, S.; Choi, D.; Kim, W. The ethylene-responsive factor like protein 1 (CaERFLP1) of hot pepper (*Capsicum annuum* L.) interacts in vitro with both GCC and DRE/CRT sequences with different binding affinities: Possible biological roles of CaERFLP1 in response to pathogen infection and high salinity conditions in transgenic tobacco plants. *Plant Mol. Biol.* **2004**, *55*, 61–81. [CrossRef] [PubMed]
48. Ahmad, A.; Niwa, Y.; Goto, S.; Ogawa, T.; Shimizu, M.; Suzuki, A.; Kobayashi, K.; Kobayashi, H. *bHLH*106 Integrates Functions of Multiple Genes through Their G-Box to Confer Salt Tolerance on Arabidopsis. *PLoS ONE* **2015**, *10*, e0126872. [CrossRef] [PubMed] [PubMed Central]
49. Bowles, D.; Lim, E.-K.; Poppenberger, B.; Vaistij, F.E. GLYCOSYLTRANSFERASES OF LIPOPHILIC SMALL MOLECULES. *Plant Biol.* **2006**, *57*, 567–597. [CrossRef] [PubMed]
50. Yang, X.; Che, Y.; García, V.J.; Shen, J.; Zheng, Y.; Su, Z.; Zhu, L.; Luan, S.; Hou, X. Cyclophilin 37 maintains electron transport via the cytochrome b6/f complex under high light in Arabidopsis. *Plant Physiol.* **2023**, *4*, 2803–2821. [CrossRef] [PubMed]
51. Hirst, J.; Itzhak, D.N.; Antrobus, R.; Borner, G.H.H.; Robinson, M.S. Role of the AP-5 adaptor protein complex in late endosome-to-Golgi retrieval. *PLoS Biol.* **2018**, *16*, e2004411. [CrossRef] [PubMed] [PubMed Central]

52. Couturier, J.; Touraine, B.; Briat, J.F.; Gaymard, F.; Rouhier, N. The iron-sulfur cluster assembly machineries in plants: Current knowledge and open questions. *Front Plant Sci.* **2013**, *24*, 259. [CrossRef] [PubMed] [PubMed Central]
53. Walters, R.G.; Shephard, F.; Rogers, J.J.; Rolfe, S.A.; Horton, P. Identification of mutants of Arabidopsis defective in acclimation of photosynthesis to the light environment. *Plant Physiol.* **2003**, *131*, 472–481. [CrossRef] [PubMed] [PubMed Central]
54. Carianopol, C.S.; Gazzarrini, S. SnRK1α1 Antagonizes Cell Death Induced by Transient Overexpression of Arabidopsis Thaliana ABI5 Binding Protein 2 (AFP2). *Front. Plant Sci.* **2020**, *11*, 582208. [CrossRef] [PubMed]
55. Yanagisawa, S. Dof Domain Proteins: Plant-Specific Transcription Factors Associated with Diverse Phenomena Unique to Plants. *Plant Cell Physiol.* **2004**, *45*, 386–391. [CrossRef] [PubMed]
56. Fornara, F.; Panigrahi, K.C.; Gissot, L.; Sauerbrunn, N.; Rühl, M.; Jarillo, J.A.; Coupland, G. Arabidopsis DOF transcription factors act redundantly to reduce CONSTANS expression and are essential for a photoperiodic flowering response. *Dev. Cell* **2009**, *17*, 75–86. [CrossRef] [PubMed]
57. Reverter, D.; Lima, C.D. Preparation of SUMO proteases and kinetic analysis using endogenous substrates. *Methods Mol. Biol.* **2009**, *497*, 225–239. [CrossRef] [PubMed] [PubMed Central]
58. Yang, P.; Smalle, J.; Lee, S.; Yan, N.; Emborg, T.J.; Vierstra, R.D. Ubiquitin C-terminal hydrolases 1 and 2 affect shoot architecture in Arabidopsis. *Plant J.* **2007**, *51*, 441–457. [CrossRef] [PubMed]
59. Murayama, M.; Hayashi, S.; Nishimura, N.; Ishide, M.; Kobayashi, K.; Yagi, Y.; Asami, T.; Nakamura, T.; Shinozaki, K.; Hirayama, T. Isolation of Arabidopsis ahg11, a weak ABA hypersensitive mutant defective in nad4 RNA editing. *J. Exp. Bot.* **2012**, *63*, 5301–5310. [CrossRef] [PubMed] [PubMed Central]
60. Uchikoba, T.; Yonezawa, H.; Kaneda, M. Cleavage specificity of cucumisin, a plant serine protease. *J. Biochem.* **1995**, *117*, 1126–1130. [CrossRef] [PubMed]
61. Ogawa, M.; Kay, P.; Wilson, S.; Swain, S.M. ARABIDOPSIS DEHISCENCE ZONE POLYGALACTURONASE1 (ADPG1), ADPG2, and QUARTET2 are Polygalacturonases required for cell separation during reproductive development in Arabidopsis. *Plant Cell* **2009**, *21*, 216–233. [CrossRef] [PubMed]
62. Wu, X.; Dabi, T.; Weigel, D. Requirement of homeobox gene STIMPY/WOX9 for Arabidopsis meristem growth and maintenance. *Curr. Biol.* **2005**, *15*, 436–440. [CrossRef] [PubMed]
63. Werner, T.; Motyka, V.; Laucou, V.; Smets, R.; Van Onckelen, H.; Schmülling, T. Cytokinin-deficient transgenic Arabidopsis plants show multiple developmental alterations indicating opposite functions of cytokinins in the regulation of shoot and root meristem activity. *Plant Cell* **2003**, *15*, 2532–2550. [CrossRef] [PubMed]
64. Ogawa, E.; Yamada, Y.; Sezaki, N.; Kosaka, S.; Kondo, H.; Kamata, N.; Abe, M.; Komeda, Y.; Takahashi, T. ATML1 and PDF2 Play a Redundant and Essential Role in Arabidopsis Embryo Development. *Plant Cell Physiol.* **2015**, *56*, 1183–1192. [CrossRef] [PubMed]
65. Ikeda, M.; Fujiwara, S.; Mitsuda, N.; Ohme-Takagi, M. A triantagonistic basic helix-loop-helix system regulates cell elongation in Arabidopsis. *Plant Cell* **2012**, *24*, 4483–4497. [CrossRef] [PubMed]
66. Taira, T.; Yamagami, T.; Aso, Y.; Ishiguro, M.; Ishihara, M. Localization, accumulation, and antifungal activity of chitinases in rye (Secale cereale) seed. *Biosci. Biotechnol. Biochem.* **2001**, *65*, 2710–2718. [CrossRef] [PubMed]
67. Herger, A.; Dünser, K.; Kleine-Vehn, J.; Ringli, C. Leucine-Rich Repeat Extensin Proteins and Their Role in Cell Wall Sensing. *Curr. Biol.* **2019**, *29*, R851–R858. [CrossRef] [PubMed]
68. Figueiredo, L.; Santos, R.B.; Figueiredo, A. Defense and Offense Strategies: The Role of Aspartic Proteases in Plant-Pathogen Interactions. *Biology* **2021**, *10*, 75. [CrossRef] [PubMed] [PubMed Central]
69. Wang, T.; Liang, L.; Xue, Y.; Jia, P.F.; Chen, W.; Zhang, M.X.; Wang, Y.C.; Li, H.J.; Yang, W.C. A receptor heteromer mediates the male perception of female attractants in plants. *Nature* **2016**, *531*, 241–244; Erratum in *Nature* **2016**, *536*, 360. [CrossRef]
70. Milla, M.A.; Townsend, J.; Chang, I.F.; Cushman, J.C. The Arabidopsis AtDi19 gene family encodes a novel type of Cys2/His2 zinc-finger protein implicated in ABA-independent dehydration, high-salinity stress and light signaling pathways. *Plant Mol. Biol.* **2006**, *61*, 13–30. [CrossRef] [PubMed]
71. Carrera, D.A.; George, G.M.; Fischer-Stettler, M.; Galbier, F.; Eicke, S.; Truernit, E.; Streb, S.; Zeeman, S.C. Distinct plastid fructose bisphosphate aldolases function in photosynthetic and non-photosynthetic metabolism in Arabidopsis. *J. Exp. Bot.* **2021**, *72*, 3739–3755. [CrossRef] [PubMed]
72. Heazlewood, J.L.; Whelan, J.; Millar, A.H. The products of the mitochondrial orf25 and orfB genes are FO components in the plant F1FO ATP synthase. *FEBS Lett.* **2003**, *540*, 201–205. [CrossRef] [PubMed]
73. Ahmad, B.; Zhang, S.; Yao, J.; Rahman, M.U.; Hanif, M.; Zhu, Y.; Wang, X. Genomic Organization of the B3-Domain Transcription Factor Family in Grapevine (*Vitis vinifera* L.) and Expression during Seed Development in Seedless and Seeded Cultivars. *Int. J. Mol. Sci.* **2019**, *20*, 4553. [CrossRef] [PubMed]
74. Funk, H.M.; Zhao, R.; Thomas, M.; Spigelmyer, S.M.; Sebree, N.J.; Bales, R.O.; Burchett, J.B.; Mamaril, J.B.; Limbach, P.A.; Guy, M.P. Identification of the enzymes responsible for m2,2G and acp3U formation on cytosolic tRNA from insects and plants. *PLoS ONE* **2020**, *15*, e0242737. [CrossRef] [PubMed] [PubMed Central]
75. Meinke, D.W. Genome-wide Identification of EMBRYO-DEFECTIVE (EMB) Genes Required for Growth and Development in Arabidopsis. *N. Phytol.* **2020**, *226*, 306–325. [CrossRef] [PubMed]
76. Chaudhry, F.; Guérin, C.; von Witsch, M.; Blanchoin, L.; Staiger, C.J. Identification of Arabidopsis cyclase-associated protein 1 as the first nucleotide exchange factor for plant actin. *Mol. Biol. Cell* **2007**, *18*, 3002–3014. [CrossRef] [PubMed] [PubMed Central]

77. Lazaridi, E.; Kapazoglou, A.; Gerakari, M.; Kleftogianni, K.; Passa, K.; Sarri, E.; Papasotiropoulos, V.; Tani, E.; Bebeli, P.J. Crop Landraces and Indigenous Varieties: A Valuable Source of Genes for Plant Breeding. *Plants* **2024**, *13*, 758. [CrossRef] [PubMed]
78. Zhang, J.; Wang, J.; Zhu, C.; Singh, R.P.; Chen, W. Chickpea: Its Origin, Distribution, Nutrition, Benefits, Breeding, and Symbiotic Relationship with Mesorhizobium Species. *Plants* **2024**, *13*, 429. [CrossRef] [PubMed]
79. Upadhyaya, H.D.; Bajaj, D.; Das, S.; Saxena, M.S.; Badoni, S.; Kumar, V.; Tripathi, S.; Gowda, C.L.L.; Sharma, S.; Tyagi, A.K.; et al. A Genome-Scale Integrated Approach Aids in Genetic Dissection of Complex Flowering Time Trait in Chickpea. *Plant Mol. Biol.* **2015**, *89*, 403–420. [CrossRef] [PubMed]
80. Wang, J.; Zhang, Z. GAPIT Version 3: Boosting Power and Accuracy for Genomic Association and Prediction. *Biorxiv* **2020**. [CrossRef]
81. Sánchez-Martín, J.; Rispail, N.; Flores, F.; Emeran, A.A.; Sillero, J.C.; Rubiales, D.; Prats, E. Higher Rust Resistance and Similar Yield of Oat Landraces versus Cultivars under High Temperature and Drought. *Agron. Sustain. Dev.* **2016**, *37*, 3. [CrossRef]
82. Rispail, N.; Montilla-Bascón, G.; Sánchez-Martín, J.; Flores, F.; Howarth, C.; Langdon, T.; Rubiales, D.; Prats, E. Multi-Environmental Trials Reveal Genetic Plasticity of Oat Agronomic Traits Associated with Climate Variable Changes. *Front. Plant Sci.* **2018**, *9*, 1358. [CrossRef] [PubMed]
83. Duk, M.A.; Kanapin, A.A.; Bankin, M.P.; Vishnyakova, M.A.; Bulyntsev, S.V.; Samsonova, M.G. Genome-Wide Association Analysis in Chickpea Landraces and Cultivars. *Biophysics* **2023**, *68*, 952–963. [CrossRef]